

Cryptography using optical chaos/Cryptographie par chaos optique

Synchronization properties of chaotic semiconductor lasers and applications to encryption

Claudio R. Mirasso^{a,b,*}, Raúl Vicente^b, Pere Colet^c, Josep Mulet^b, Toni Pérez^b

^a Department of Electrical Engineering, 56-147C Engineering IV, UCLA, Los Angeles, CA 90095-159410, USA

^b Departament de Física, Universitat de les Illes Balears, 07122 Palma de Mallorca, Spain

^c Instituto Mediterráneo de Estudios Avanzados (IMEDEA) CSIC-UIB, Campus UIB, 07122 Palma de Mallorca, Spain

Presented by Guy Laval

Abstract

We review the main properties of two unidirectionally coupled single-mode semiconductor lasers (*master-slave* configuration). Our analysis is based on numerical simulations of a rate equations model. The emitter, or master laser, is assumed to be an external-cavity single-mode semiconductor laser subject to optical feedback that operates in a chaotic regime. The receiver, or slave laser, is similar to the emitter but can either operate in a chaotic regime, as the emitter (closed loop configuration), or without optical feedback and consequently under CW when it is uncoupled (open loop configuration). This configuration is one of the most simple and useful configuration for chaos based communication systems and data encryption. **To cite this article:** *C.R. Mirasso et al., C. R. Physique 5 (2004).*

© 2004 Académie des sciences. Published by Elsevier SAS. All rights reserved.

Résumé

Un système cryptographique à laser à semi-conducteurs à courte cavité. Les principales propriétés de couplage unidirectionnel entre deux laser à semi-conducteurs monomodes (configuration *maître-esclave*) sont passées en revue. Cette analyse s'appuie sur des simulations numériques du modèle des équations d'évolution du laser à semi-conducteur. L'émetteur, ou encore le laser maître, est constitué d'un laser semi-conducteur monomode à cavité externe soumis à une contre-réaction optique, et fonctionnant en régime chaotique. Le récepteur, ou laser esclave, est semblable à l'émetteur, mais il peut fonctionner soit en régime chaotique comme l'émetteur (configuration en boucle fermée), soit sans contre-réaction optique (configuration en boucle ouverte), c'est-à-dire en régime continu lorsqu'il est non couplé. Cette dernière configuration est l'une des plus simples et des plus communes dans le contexte des systèmes de sécurisation des télécommunications optiques par chaos. **Pour citer cet article :** *C.R. Mirasso et al., C. R. Physique 5 (2004).*

© 2004 Académie des sciences. Published by Elsevier SAS. All rights reserved.

Keywords: Synchronization; Chaos; Chaos encryption; Optical chaos communications; Semiconductor lasers

Mots-clés : Synchronisation ; Chaos ; Cryptographie par chaos ; Télécommunications optiques par chaos ; Lasers semi-conducteurs

1. Introduction

At the beginning of the last decade, Pecora and Carroll [1] published the first studies on the dynamical properties of two coupled chaotic systems and reported that under certain conditions two chaotic systems could synchronize [2]. Cuomo and

* Corresponding author.

E-mail address: claudio@imedea.uib.es (C.R. Mirasso).

Oppenheim [3] proposed in 1993 to use two synchronized chaotic circuits for encrypted communication purposes. After these works, the possibility of using chaos synchronization to encode information has been receiving much attention. As already mentioned, the first experiments were carried out using electronic circuits, such as Lorenz or Chua circuits. However, such systems present two disadvantages: on the one hand the maximum frequency for the chaotic carriers is some tens of KHz and, on the other hand, the dimensionality of the generated chaos is low (typically less than 3), and consequently message confidentiality is not very high.

It was already clear in 1994 that the optical domain could overcome some of the previously mentioned disadvantages. The first proposal was done using solid state lasers [4], although a breakthrough occurred when the use of semiconductor lasers subject to delayed feedback was suggested. Semiconductor lasers are inherently non-linear devices, fast and easy to modulate and under chaotic operation its broad spectrum can extend over some tens of GHz. Based on these ideas, it was numerically shown that Gbit/s messages could be encoded and decoded within a highly dimensional chaotic carrier when using a pair of unidirectionally coupled semiconductor lasers subject to coherent optical feedback or injection [5–7]. Experimental results were later obtained for Erbium doped fiber ring lasers [8], semiconductor lasers [9–11] and microchip lasers [12]. More recently, it was also shown that the system would also work when using incoherent optical feedback [13] or optoelectronic feedback [14–17].

Many studies have already been carried out to check the robustness of the synchronized systems [18–22] in both the closed and open loop configuration (i.e., when the receiver systems is subjected or not to its own feedback loop). Most of them indicate that a mismatch in parameters up to $\sim 5\%$ would still allow for synchronization and message recovery what confirms the possibility of using these ideas in real systems where unavoidable fabrication mismatches occur.

In this work we numerically study the synchronization and the message encoding in both closed and open loop schemes, and their performance is compared in order to determine the advantages and disadvantages of each configuration. We can anticipate that in most of the cases the closed loop scheme has a better performance than the open one, although the latter requires a careful adjustment of both external cavities to operate correctly. In Section 2 we present the model; Section 3 is devoted to the results concerning the characterization of the chaos while the synchronization properties of the system are reviewed in Section 4. Section 5 collects a comparison of the different schemes regarding message recovery performance. A summary and some conclusions are given in Section 6.

2. Model and parameters

We study the synchronization between two single-mode semiconductor lasers in a master-slave configuration (see Fig. 1). We model the feedback effect in the transmitter and receiver lasers by using the well-known Lang–Kobayashi description [23] for the complex slowly-varying amplitude of the electrical field $E_{t,r}$ and the carriers number inside the cavity $N_{t,r}$. With the assumption of a free link between both lasers and the introduction of the symmetric reference frame $\Omega = (\omega_t + \omega_r)/2$, $\Delta\omega = \omega_t - \omega_r$, these equations are written as [21]:

$$\dot{E}_{t,r}(t) = \pm \frac{i\Delta\omega}{2} E_{t,r} + \frac{1+i\alpha}{2} \left[G_{t,r} - \frac{1}{\tau_{ph}} \right] E_{t,r} + \kappa_{t,r} E_{t,r}(t - \tau_f) e^{-i\Omega\tau_f} + \kappa_c E_t(t - \tau_c) e^{-i\Omega\tau_c}, \tag{1}$$

$$\dot{N}_{t,r}(t) = \frac{I_{t,r}}{e} - \frac{N_{t,r}}{\tau_n} - G_{t,r} P_{t,r}(t), \tag{2}$$

$$G_{t,r}(t) = \frac{g(N_{t,r} - N_o)}{1 + s P_{t,r}(t)} \tag{3}$$

where subscripts t, r correspond to the transmitter or master laser (ML) and receiver or slave laser (SL). The above model is adequate for small amounts of feedback and injection. The term $\kappa_c e^{-i\Omega\tau_c} E_t(t - \tau_c)$ only appears for the SL and accounts for the amount of ML output power that is injected into the SL. $P_{t,r}(t) = |E_{t,r}(t)|^2$ is the optical intensity or number of

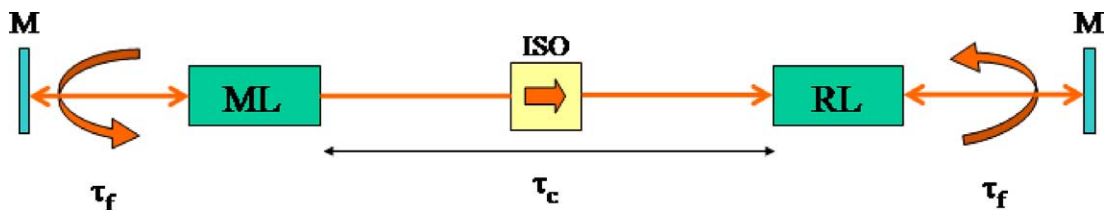


Fig. 1. Scheme of unidirectionally coupled lasers subject to coherent optical feedback.

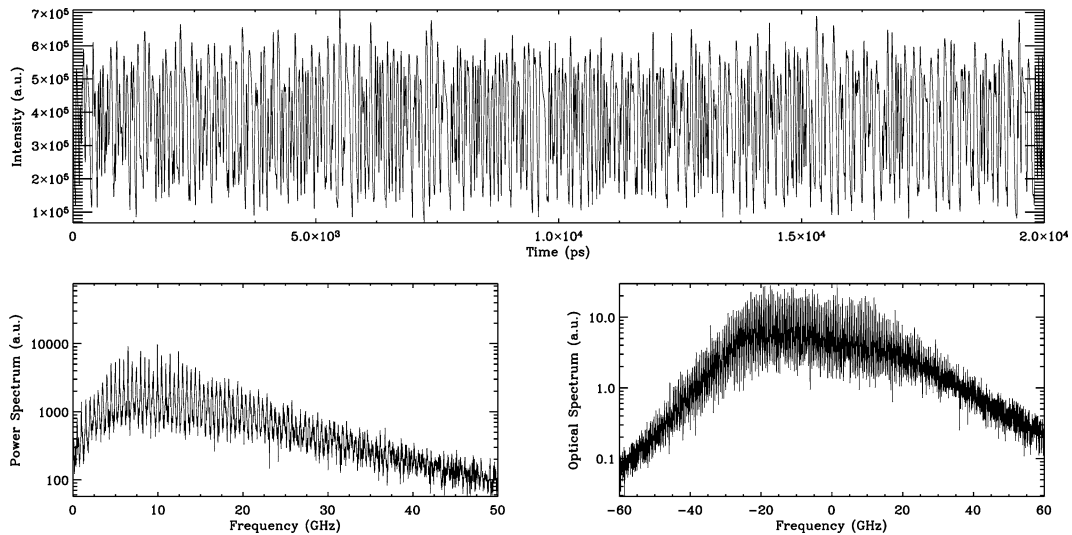


Fig. 2. At the top of the figure is represented a typical time trace of the photon number of the transmitter laser subject to optical feedback. At the left and right bottom the power and optical spectra are plotted, respectively.

photons in the cavity. We consider both lasers very similar to each other and consequently we take initially the same parameter values: $\alpha = 5$ is the linewidth enhancement factor, $g = 1.5 \times 10^{-8} \text{ ps}^{-1}$ is the gain parameter, $s = 5 \times 10^{-7}$ is the gain saturation coefficient, $\tau_{\text{ph}} = 2 \text{ ps}$ is the photon lifetime, $\tau_n = 2 \text{ ns}$ is the carrier lifetime, $N_o = 1.5 \times 10^8$ is the carrier number at transparency, $e = 1.602 \times 10^{-19} \text{ C}$ is the electronic charge, $\omega_{t,r}$ is the frequency of the free running laser, $\Delta\omega = \omega_t - \omega_r$ is the detuning between the optical frequencies of the lasers, $\kappa_{t,r}$ is the feedback coefficient, κ_c is the coupling rate, τ_f is the external cavity round-trip time and τ_c is the time the light it takes to travels from the ML to SL. For this internal parameters, the threshold current amounts to $I_{\text{th}} \approx 14.7 \text{ mA}$.

We consider two possible situations for the system: one in which the ML is subjected to a coherent optical feedback and operates in the coherence collapse regime while the SL operates under CW (open loop scheme) when they are uncoupled. For the second situation we consider both ML and SL subject to a coherent optical feedback (closed loop scheme). In both schemes, only the light coming from the transmitter laser is injected into the receiver one.

In Fig. 2, we plot a typical time trace and the power and optical spectra of the output of the emitter laser for a typical situation. The laser is biased at three times threshold, the feedback strength is 30 ns^{-1} while the feedback delay time is set to 2 ns. For this parameters the laser is operating in the coherence collapse regime, a dynamical state widely studied both numerically and experimentally [24–26]. It can be clearly seen the irregular evolution of the optical power together with a wide spectrum, clear signatures of a chaotic signal.

3. Characterization of the emitter chaos

Besides the codification scheme used to include a message in the chaotic carrier, the security of the data encryption using chaos methods relies upon two important characteristics: the unpredictability of the carrier signal, and the sensibility exhibited by the dynamics of the chaotic systems under parameter mismatch. Due to the second, only a system very similar to the chaotic transmitter can be used to decode the message in an efficient way. From a practical point of view an exhaustive study of the first characteristic is required to guarantee the security of our transmission, since it is known that low dimensional chaos would make easy the interception of the message.

We compute the Lyapunov exponents, the Kaplan–Yorke dimension and the Kolmogorov–Sinai entropy [27–29] from the Lang–Kobayashi description of the dynamics of semiconductor lasers with coherent optical feedback [30]. A chaotic behavior can be characterized by the geometrical structure of the associated attractor. There are several ways to measure the dimension of these chaotic attractors. The most common is the Hausdorff dimension, which can be measured using a box counting method [27–29]. The information dimension is a measure of the degree of disorder of the points on the attractor. More precisely, it accounts for the amount of information needed to locate the system in the phase space with infinitesimal accuracy [28]. The Hausdorff dimension is at least as large as the information dimension. A direct measurement of the Hausdorff, or the information, dimension becomes impractical for high dimensional attractors, as is the case for the systems considered here.

Therefore, we measure the Kaplan–Yorke dimension, which is conjectured to be identical to the information dimension [28], and can be calculated directly from the Lyapunov exponents. Finally, the Kolmogorov–Sinai entropy measures the average loss of information rate, or, equivalently is inversely proportional to the time interval over which the future evolution of the system can be predicted. The Kolmogorov–Sinai entropy can be related to the sum of the positive Lyapunov exponents through the Pesin’s identity [28]. For the purpose of using a chaotic carrier for encoding a message, a large value of the entropy, and therefore a short carrier predictability time, should yield a better masking and an improvement of the security.

In the following, we will analyze the dependence of these chaos quantifiers on the feedback parameters, namely, the feedback strength κ , the delay time τ and the feedback phase $\Phi \equiv \Omega\tau \text{ mod}(2\pi)$. This phase can be changed from 0 to 2π by changing the round-trip cavity length within one optical wavelength, which practically implies a negligible change in τ . Therefore, in practice the feedback phase and the cavity length can be adjusted independently. As a general comment we can say that the effect of the phase on the quantities under study is only relevant in the short cavity regime (external cavity frequency \gg relaxation oscillations frequency) where the Lyapunov exponents depend in a irregular way on the specific phase value, while they are insensitive for cavities ranging in the long cavity regime (external cavity frequency \ll relaxation oscillations frequency).

For the computation of the Lyapunov exponents we have applied the ideas of Farmer [29] to our case, integrating the corresponding delay differential equations with an Adams–Bashforth–Moulton fourth order predictor-corrector method.

3.1. Information dimension

As it was above mentioned, the computation of the information dimension will be estimated from the Kaplan–Yorke formula

$$d_{KY} = j + \frac{\sum_{i=1}^j \lambda_i}{|\lambda_{j+1}|}, \tag{4}$$

where the integer j , that represents the number of degrees of freedom, meets the conditions $\sum_{i=1}^j \lambda_i > 0$ and $\sum_{i=1}^{j+1} \lambda_i < 0$ when the Lyapunov exponents are ordered by their magnitude from positive to negative values.

We first analyze the value of the information dimension as function of the feedback strength κ and delay time τ . In Fig. 3 are represented the information dimension as function of κ for $\tau = 200, 300$ and 1000 ps in the case where the pump is set to

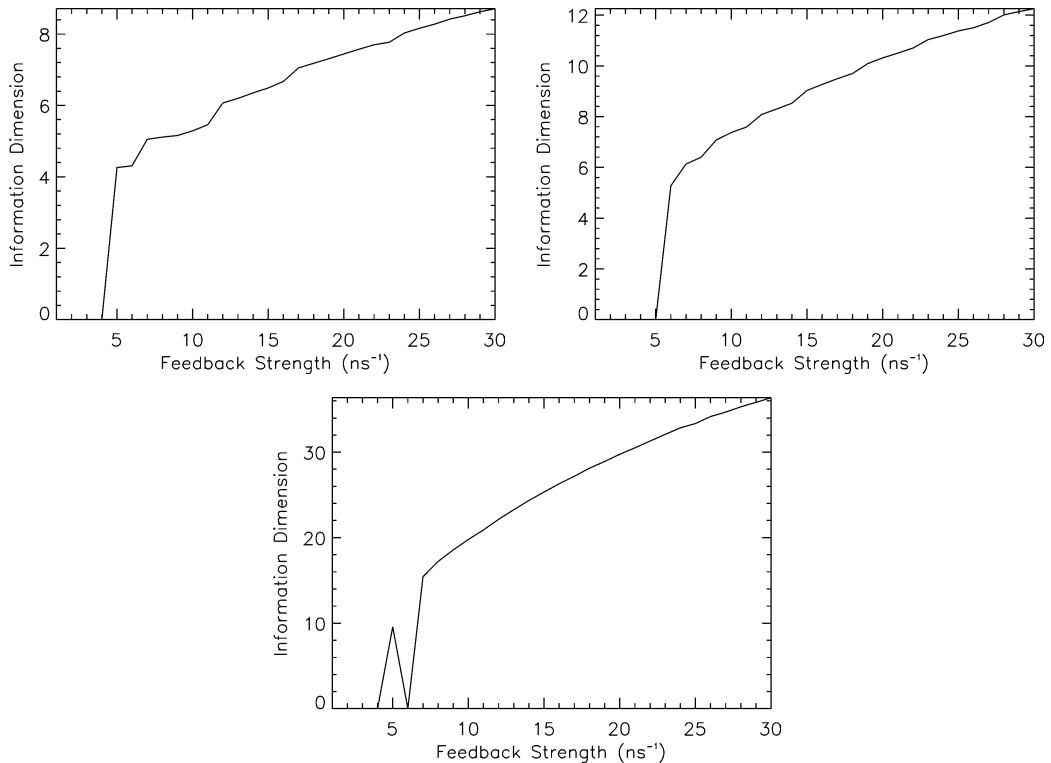


Fig. 3. Information dimension as a function of the feedback for pump $I = 1.5I_{th}$. From left to right, $\tau = 200, 300$ and 1000 ps.

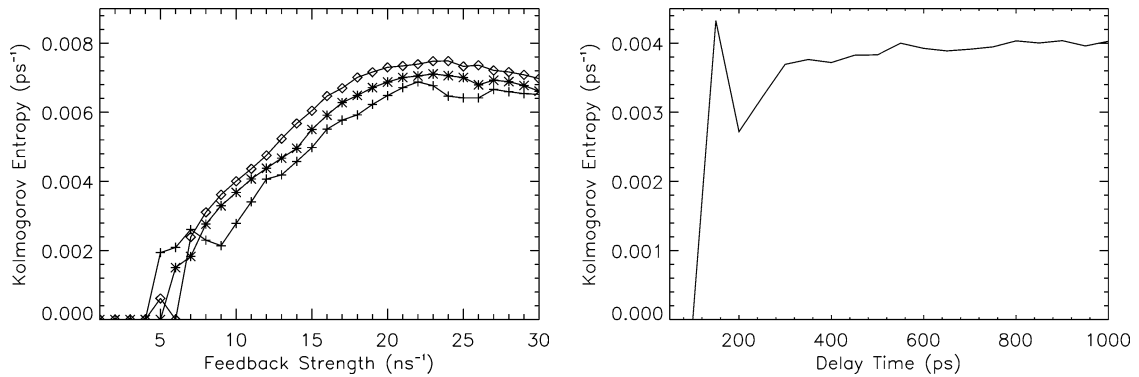


Fig. 4. (Left) Kolmogorov–Sinai entropy as function of the feedback strength for delay times $\tau = 200$ ps (crosses), 300 ps (asterisks) and 1000 ps (diamonds). (Right) Kolmogorov–Sinai entropy as function of the delay time for $\kappa = 10$ ns⁻¹.

1.5 times the threshold. Note that at this pump, the frequency of the relaxation oscillations is about 4.1 GHz and therefore, with the former range of values considered for the delay time, we are both exploring the situations of short and long cavity regimes.

We have also checked that for very short external cavities ($\tau = 100$ ps) the behavior of the information dimension as function of the feedback strength is quite irregular and at most only one positive exponent is obtained. In this regime there is also a strong dependence on the phase of the feedback. However, for longer cavities as we can observe in Fig. 3, the behavior is much more regular. After a critical value of κ where the fixed point solution ($d_{KY} = 0$) loses its stability, a rapid growing of the dimension is observed before a linear growth with the feedback strength is achieved. In terms of the Lyapunov spectrum, what is observed is that although more positive Lyapunov exponents arise as the feedback strength is increased, their magnitude decreases leading to a linear growing of the information dimension for feedback and delay values large enough. This behavior will have significant consequences in the Kolmogorov–Sinai entropy.

3.2. Kolmogorov–Sinai entropy

The computation of the Kolmogorov–Sinai entropy is again obtained from the Lyapunov exponents, through the so-called Pesin identity that states

$$h_{KS} = \sum_{i|\lambda_i > 0} \lambda_i, \quad (5)$$

i.e., the Kolmogorov–Sinai entropy is equal to the sum of all the positive Lyapunov exponents. To be precise, the sum of the positive Lyapunov exponents is an upper bound to the Kolmogorov–Sinai entropy but the equality (5) seems to hold in very general situations and it is usually the only way to obtain a good estimation of h_{KS} .

Fig. 4(left) shows the Kolmogorov–Sinai entropy as function of the feedback strength for a pumping of $I = 1.5I_{th}$. The different symbols correspond to different delay times (200, 300 and 1000 ps). The three curves basically coincide, what indicates the saturation of the entropy with the delay time, as it is clearly shown in Fig. 4(right). As happens in the case of electro-optical feedback [31,30], longer delays increase the information dimension (we have more positive Lyapunov exponents); however, as their value becomes smaller, the Kolmogorov–Sinai entropy remains basically constant.

Thus, the conclusion here is that it is not easy to increase the value of the entropy. For a given pump value, increasing the feedback level beyond an optimal value leads to a decreasing entropy. On the other hand, for a given feedback strength, increasing the delay time leads to a saturation value for the entropy.

Therefore, although the system has a larger dimensionality when increasing the delay, its behaviour does not become more unpredictable. Consequently, for the purpose of using this chaotic output as a carrier for encoding a message, these results suggest that increasing the delay time or feedback strength beyond the value at which the entropy saturates will neither yield a better masking nor improve the security.

4. Synchronization properties

4.1. Open versus closed loop configurations

In this section, we numerically study the synchronization quality of the system in terms of the coupling strength κ_c and feedback rates $\kappa_{t,r}$ for both the open and closed loop configurations, maintaining the same parameters for both transmitter and

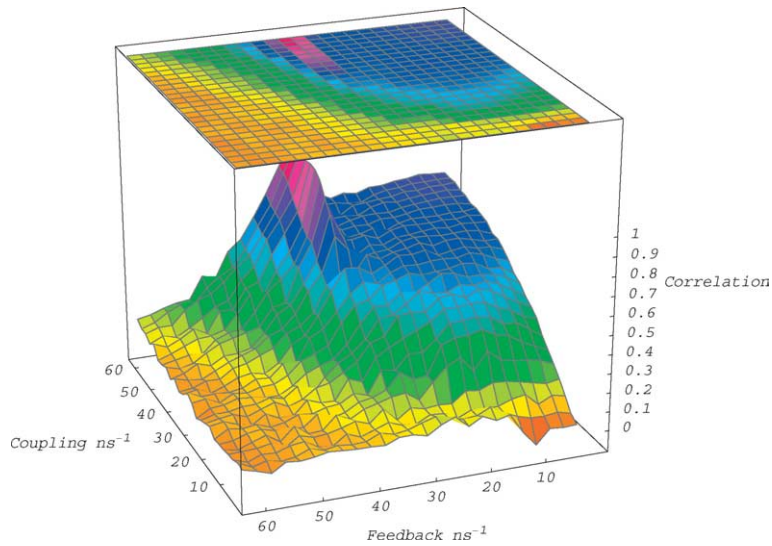


Fig. 5. Synchronization regions in the coupling–feedback parameter space for the generalized solution.

receiver lasers. The measurement of the degree of synchronization and the lag time between the time series is accomplished with the computation of the cross-correlation function

$$\Gamma(s) = \frac{\langle (P_t(t) - \langle P_t \rangle)(P_r(t+s) - \langle P_r \rangle) \rangle}{\sqrt{\langle (P_t(t) - \langle P_t \rangle)^2 \rangle \langle (P_r(t) - \langle P_r \rangle)^2 \rangle}} \tag{6}$$

Different types of synchronization have been found in coupled chaotic systems: identical synchronization, generalized synchronization, phase synchronization or lag synchronization [32]. Recently, two of these kinds of synchronization have been identified in unidirectionally coupled chaotic external-cavity semiconductor lasers [19]. The first type is related to the so called isochronous or generalized synchronization $P_r(t) = aP_t(t - \tau_c)$ [20] while the second is related to the lag synchronization $P_r(t) = P_t(t - \tau_c + \tau_f)$ (in this case it is also known as the anticipating solution) [33–35]. These two types of synchronization have been studied recently in terms of parameters mismatches between emitter and receiver [36].

In this work we concentrate in the generalized synchronization. It happens that the anticipating synchronization, although it is an exact solution of Eqs. (1)–(3), is hard difficult to find experimentally since even tiny parameter mismatch prevents that solution being observed. Consequently, it is less useful for chaos communications since it would require very similar components for emitter and receiver, difficult to obtain even when choosing devices grown on the same wafer.

We start our study by looking at the generalized synchronized solution and its dependence with the feedback rate and coupling strength. In the numerical simulations, the κ_c and κ_r coefficients are varied in the range 0–60 ns⁻¹ at intervals of 2.5 ns⁻¹, while the rest of the external parameters ($I_{t,r}$, $\omega_{t,r}$, κ_t) are fixed. Fig. 5 shows the results obtained for the correlation coefficient $\Gamma(-\tau_c + \tau_f)$ in the parameter space (κ_c , κ_r). The synchronization domain extends over the line $\kappa_t = \kappa_r$ and a high injection rate is needed to guarantee the stability of the solution. It has to be noted that the length of the external cavities (external cavity round-trip times) have been perfectly matched to obtain a high degree of correlation. Even for lengths that differ in a fraction of the emission wavelength, the synchronization can be completely lost, remarking the necessity of a careful control of the cavities size [37]. When the system operates out of the optimal conditions ($\kappa_t = \kappa_r$, $\kappa_c > \kappa_{t,r}$), a strong degradation of the synchronization occurs. From the inspection of the cross-correlation function we can also confirm that there are no lag solutions other than the isochronous and the identical one in the regions of the parameter space we have studied. It is important to note that the isochronous solution, the one usually observed experimentally, also occurs for the open loop case (when the SL feedback coefficient is zero in Fig. 5). However, even for the maximum coupling considered in Fig. 5 (60 ns⁻¹) the value of the $\Gamma(-\tau_c)$ is only around 0.7 for this case. We have checked that a larger coefficient is necessary to reach a good synchronization degree, in agreement with other studies [36].

We have also computed the minimum coupling coefficient necessary to reach a correlation coefficient of 0.9 in both the open and closed loop as a function of the feedback delay time and feedback strength of the transmitter laser. The feedback strength of the receiver laser is fixed to be $\kappa_r = \kappa_t$ for the closed loop and $\kappa_r = 0$ for the open loop. Fig. 6 shows the results of the numerical simulations. The upper surface correspond to the open loop regime while the lower one is obtained for the closed loop case. We observe that this minimum coupling is in all cases independent of the delay time and it increases with the feedback strength. In general, the coupling needs to be very large although it is clearly smaller in the closed loop case.

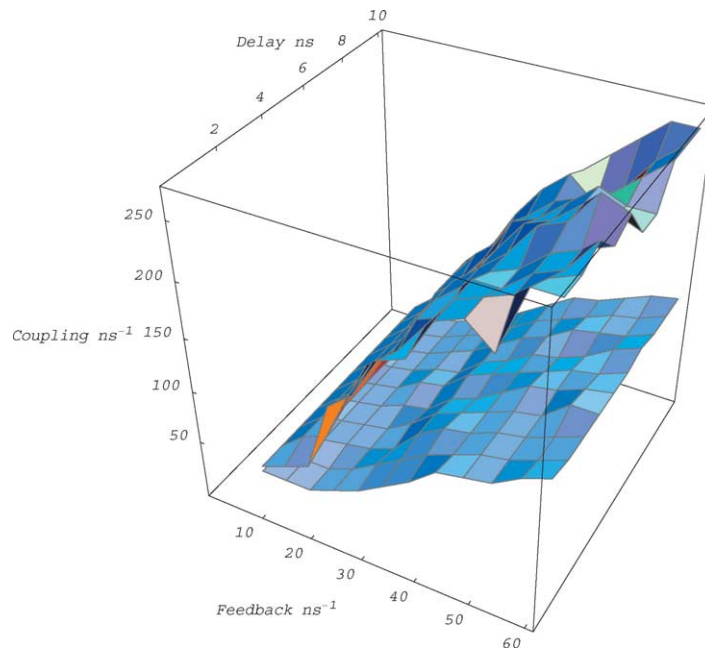


Fig. 6. Minimum coupling necessary to get a correlation value of 0.9 as function of the delay feedback time and the feedback strength in the transmitter. Upper and lower surfaces stand for the open and closed loop schemes, respectively.

4.2. Parameter mismatch

In Figs. 5 and 6, it has been shown that the degree of synchronization approaches to 1, in both open and closed loop configurations, beyond a given coupling strength for an identical pair of emitter-receiver lasers. However, this situation is unrealistic since any two lasers, even obtained from the same wafer, have a certain mismatch. Consequently, we need to study the degree of synchronization for a certain mismatch between emitter and receiver. In the following, we show how the correlation coefficient between the two laser outputs varies, as function of some parameter mismatches for the generalized synchronization, in both open and closed loop configurations. The receiver laser parameters have been changed with respect to the values given in the text by multiplying them by a factor $(1 + \delta/100)$ being δ the relative percentage of change. The left and right panels in Fig. 7 represent the results of the maxima of the cross correlation coefficient for the close and open loops, respectively.

In this case, we have chosen the long cavity regime $\tau_f = 1$ ns, $\kappa_f = 30$ ns⁻¹ and $\kappa_c = 180$ ns⁻¹ for the open loop configuration while the coupling strength is fixed to 60 ns⁻¹ for the closed loop configuration. It can be immediately noticed that the generalized synchronization, either within the open or closed loop, is not extremely sensitive to parameter mismatches. Correlation coefficients close to 1 can be obtained for a range of parameter mismatch $> 20\%$ for the open loop while a smaller range is obtained for the closed loop. These results are in qualitative agreement with the experimental observations that synchronization within the closed loop scheme is only obtained for very similar lasers. For the operation regime here considered (3 times threshold and long cavity limit), it seems that the photon lifetime, differential gain and saturation are the most critical parameters for the closed loop scheme. In general, there is a tendency, more noticeable for the closed loop scheme that tells us that the synchronization quality exhibits an asymmetric behavior with respect to the sign of the parameter mismatch. Part of this asymmetry can be explained by the compensation that some parameter mismatches are able to perform on the increase of optical power in the receiver laser due to the injection term.

5. Encoding/decoding schemes

In this section we briefly study the performance of the message encoding/decoding process when using two of the most widely used techniques: chaos shift keying (CSK) and chaos modulation (CM). Although other methods have been also proved successful such as chaos masking (CMA), on-off chaos shift keying (OOCSSK) or on-off phase shift keying (OOPSK), the two schemes we study here are probably the easiest to implement in a real system. In the CSK technique, the information is introduced into the transmitter by slightly modulating the injection current of the laser with the message one wants to transmit.

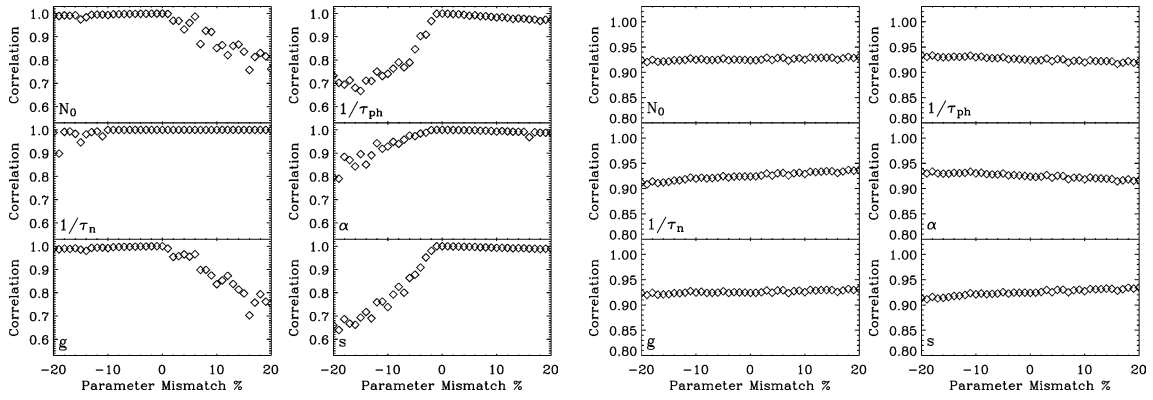


Fig. 7. Left panel: parameter mismatch effect on the synchronization quality for the closed loop configuration. Right panel: parameter mismatch effect on the synchronization quality for the open loop configuration. The symbol insets in the graphics indicate the parameter mismatch that has been induced.

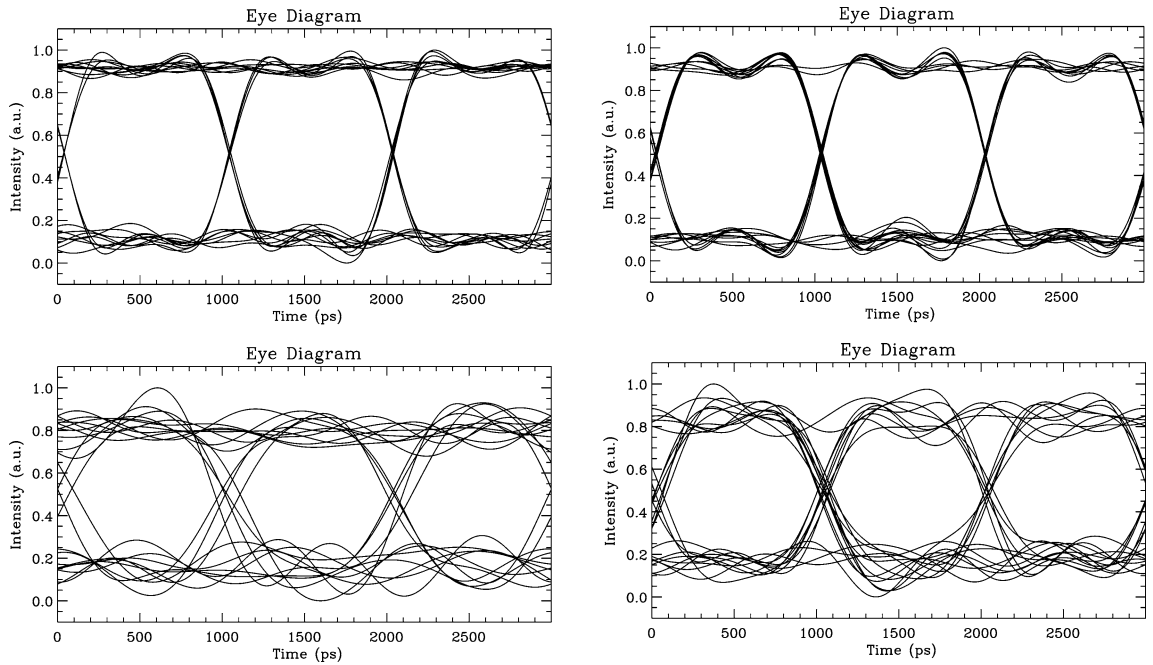


Fig. 8. Eye diagrams for the CSK codification technique at 0.5 Gbit/s (left panel) and 1 Gbit/s (right panel). Upper diagrams are for the closed loop scheme while the lower ones contain the results corresponding to the open loop scheme.

It is the easiest way to encode information and has been used for decades to generate optical pulses. In the CM technique, the chaotic carrier is modulated by the message at the transmitter laser output. This technique requires the use of an external modulator driven by the message.

For simplicity, we consider here identical parameters and operating conditions for the emitter and receiver systems. After the transmission of a given message, the quality of the recovery can be estimated by looking at the eye patterns obtained through the corresponding message decryption process.

The encoded message was a $2^6 - 1$ pseudorandom non-return to zero (NRZ) bit sequence. In Fig. 8 we show the eye diagram of the recovery message, obtained for the CSK encoding at 0.5 Gbit/s and 1 Gbit/s for the closed (upper panels) and open loop (lower panels) schemes. The modulation index is set to 5%. As expected, the quality of the eye diagrams is better for the closed loop scheme although those for the open loop have good quality for both bit rates.

In Fig. 9 we show the eye diagram obtained for the CM encoding at 0.5 Gbit/s and 1 Gbit/s for the closed loop scheme. The modulation index is also fixed to 5%. For this encoding technique, numerical simulations have confirmed that the open

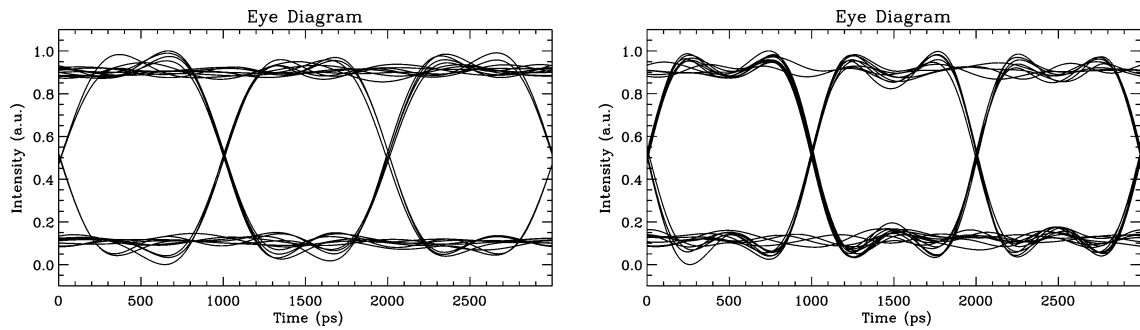


Fig. 9. Eye diagrams for the CM codification technique at 0.5 Gbit/s (left panel) and 1 Gbit/s (right panel).

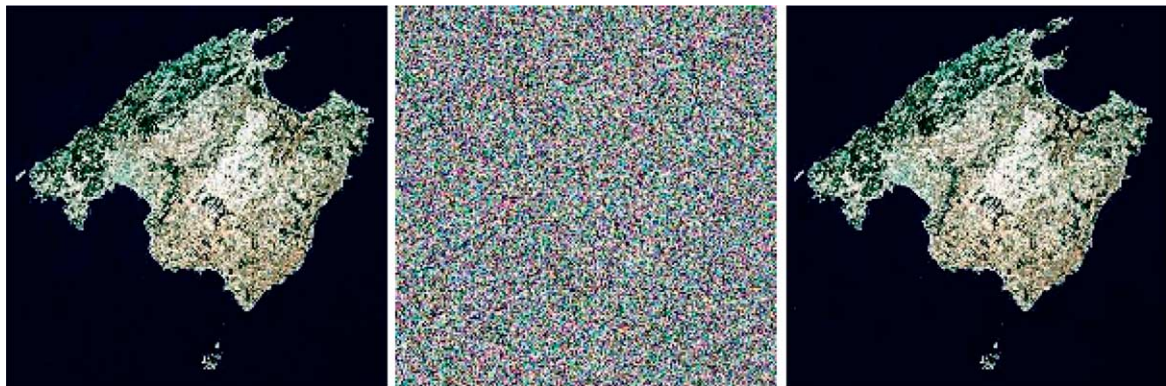


Fig. 10. Image transmission and recovery at 1 Gbit/s. CSK codification scheme has been used.

loop configuration seems to be unable to recover the message unless an extremely high coupling strength is allowed. This large coupling might be obtained by, e.g., amplifying and filtering the signal when injecting it into the receiver. However, since the effects of the amplification processes require a detailed study (see, e.g., [38,39]), out of the scope of this paper, CM encoding in the open loop scheme has not been considered here.

As a final graphical example, we show in Fig. 10 the encoding/decoding of a picture of the Island of Mallorca, using the CSK scheme. The left panel corresponds to the original image, the middle panel to the image that an eavesdropper would see if he taps the transmission and the right panel corresponds to the recovered image. The recovery of the image looks (at least at first sight) almost perfect.

6. Summary and conclusions

We have studied the synchronization properties of two unidirectionally coupled single mode semiconductor lasers. These devices are interesting, not only for their fundamental aspects, but also as sources for optical chaos communication systems. For the latter, a high dimensional and complex chaotic carrier is required to ensure the privacy of the encrypted information. We have characterized the dimension and the entropy of the chaotic carriers by means of Lyapunov exponents, Kaplan–York dimension and the Kolmogorov–Sinai entropy. We found a saturation of the latter with the feedback cavity length and strength, which indicates the existence of an optimum value for this two parameters. We have also studied the synchronization quality under parameter mismatch and compared open versus closed loop performance. We found that open loop scheme is less sensitive to parameter mismatch than the closed loop scheme. Chaos shift keying and chaos modulation have been shown as examples of message encryption techniques. We found that closed loops receivers show better performance for extracting the message. In fact for chaos modulation, the message can only be recovered by using closed loop receivers.

Acknowledgements

This work was supported by the OCCULT project (IST-2000-29683) and the Spanish MCyT and FEDER projects CONOCE BFM2000-1108, SINFIBIO BMF2001-0341 and BFM2002-04369.

References

- [1] L.M. Pecora, T.L. Carroll, *Phys. Rev. Lett.* 64 (1990) 821.
- [2] L.M. Pecora, T.L. Carroll, *Phys. Rev. A* 44 (1991) 2374.
- [3] K.M. Cuomo, A.V. Oppenheim, *Phys. Rev. Lett.* 71 (1993) 65.
- [4] P. Colet, R. Roy, *Opt. Lett.* 19 (1994) 2056.
- [5] C.R. Mirasso, P. Colet, P. Garcia-Fernandez, *IEEE Photon Technol. Lett.* 8 (1996) 299.
- [6] V. Annovazzi-Lodi, S. Donati, A. Scire, *IEEE J. Quantum Electron.* 32 (1996) 953.
- [7] K. White, J. Moloney, *Phys. Rev. A* 59 (1998) 2422.
- [8] G.D. VanWiggeren, R. Roy, *Science* 279 (1998) 1198.
- [9] L. Larger, J.P. Goedgebuer, F. Delorme, *Phys. Rev. E* 57 (1998) 6618.
- [10] S. Sivaprakasam, K.A. Shore, *Opt. Lett.* 24 (1999) 466.
- [11] I. Fischer, Y. Liu, P. Davis, *Phys. Rev. A* 62 (2000) 011801.
- [12] A. Uchida, T. Ogawa, F. Shinozuka, M. Kannari, *Phys. Rev. E* 62 (2000) 1961.
- [13] F. Rogister, A. Locquet, D. Pieroux, M. Sciamanna, O. Deparis, P. Megret, M. Blondel, *Opt. Lett.* 26 (2001) 1486.
- [14] S. Tang, H.F. Chen, J.M. Liu, *Opt. Lett.* 26 (2001) 1489.
- [15] S. Tang, J.M. Liu, *Opt. Lett.* 26 (2001) 1843.
- [16] J.-M. Liu, H.-F. Chen, S. Tang, *IEEE J. Quantum Electron.* 38 (2002) 1184.
- [17] S. Tang, J.M. Liu, *IEEE J. Quantum Electron.* 39 (2003) 708.
- [18] A. Sanchez-Diaz, C.R. Mirasso, P. Colet, P. Garcia-Fernandez, *IEEE J. Quantum Electron.* 35 (1999) 292.
- [19] A. Locquet, F. Rogister, M. Sciamanna, M. Megret, P. Blondel, *Phys. Rev. E* 64 (2001) 045203.
- [20] J. Revuelta, C.R. Mirasso, P. Colet, L. Pesquera, *IEEE Photon. Technol. Lett.* 14 (2002) 140.
- [21] C.R. Mirasso, J. Mulet, C. Masoller, *IEEE Photon. Technol. Lett.* 14 (2002) 456.
- [22] R. Vicente, T. Perez, C.R. Mirasso, *IEEE J. Quantum Electron.* 37 (2002) 1198.
- [23] R. Lang, K. Kobayashi, *IEEE J. Quantum Electron.* 16 (1980) 347.
- [24] D. Lenstra, B. Verbeek, A. Den Boef, *IEEE J. Quantum Electron.* 21 (1985) 674.
- [25] J. Cohen, D. Lenstra, *IEEE J. Quantum Electron.* 25 (1989) 1143.
- [26] J. Cohen, D. Lenstra, *IEEE J. Quantum Electron.* 27 (1991) 10.
- [27] J. Eckmann, D. Ruelle, *Rev. Mod. Phys.* 57 (1985) 617.
- [28] H. Kantz, T. Schreiber, *Nonlinear Time Series Analysis*, Cambridge University Press, 2000.
- [29] J.D. Farmer, *Physica D* 4 (1982) 366.
- [30] R. Vicente, J. Dauden, P. Colet, R. Toral, in: *Physics and Simulation of Optoelectronic Devices XI*, in: *SPIE Proc.*, vol. 4986, 2003, p. 452.
- [31] J.P. Goedgebuer, L. Larger, H. Porte, *Phys. Rev. Lett.* 80 (1998) 2249.
- [32] S. Boccaletti, L.M. Pecora, A. Pelaez, *Phys. Rev. E* 63 (2001) 0662191.
- [33] C. Masoller, *Phys. Rev. Lett.* 86 (2001) 2782.
- [34] H.U. Voss, *Phys. Rev. E* 61 (2000) 5115.
- [35] S. Sivaprakasam, E.M. Shahverdiev, P.S. Spencer, K.A. Shore, *Phys. Rev. Lett.* 87 (2001) 0154101.
- [36] A. Locquet, C. Masoller, C. Mirasso, *Phys. Rev. E* 65 (2002) 56205.
- [37] T. Heil, J. Mulet, I. Fischer, C. Mirasso, M. Peil, P. Colet, W. Elsässer, *IEEE J. Quantum Electron.* 38 (2002) 1162.
- [38] D. Kanakidis, A. Argyris, D. Syvridis, *IEEE J. Lightwave Tech.* 21 (2003) 750.
- [39] A. Argyris, D. Syvridis, *IEEE J. Lightwave Tech.*, 2004, in press.